Phylogeny, taxonomy and life cycle of Diderma brasiliensis (Physarales, Didymiaceae): a new species of myxomycete

Lucca Araujo Toschi

lucca.toschi.bio@gmail.com

Universidade Estadual de Goias - Campus de Ciencias Exatas e Tecnologicas Henrique Santillo
https://orcid.org/0000-0002-6106-5081

Lucas Leonardo-Silva

Universidade Estadual de Goias - Campus de Ciencias Exatas e Tecnologicas Henrique Santillo

Solange Xavier-Santos

Universidade Estadual de Goias - Campus de Ciencias Exatas e Tecnologicas Henrique Santillo

Research Article

Keywords: Cultivation, dark spores, myxodiversity, new taxa, ribosomal RNA

Posted Date: August 13th, 2025

DOI: https://doi.org/10.21203/rs.3.rs-7222482/v1

Abstract

Diderma brasiliensis was found during a myxodiversity survey in Central Brazil, occurring abundantly on decomposing fallen trunks, leaf litter, and on the stems and leaves of the climbing plant *Epipremnum aureum*. It has globose to subglobose sporophores with reticulate spores and tortuous capillitia with nodular insertions, the latter two being very distinctive features of the species. In addition to these unique morphological traits, the proposal of this new species is phylogenetically supported by the 18S rRNA and mtSSU DNA regions. We also investigated its life cycle and cultivation strategies, recording the different stages of development and behavior, and we report a possible predatory interaction between the plasmodium of D. brasiliensis and the fungus Fusarium cf. decemcellulare. Although it shares similarities with other species of the genus, such as *D. cor-rubrum*, *D. crustaceum*, and *D. subdictyospermum*, *D. brasiliensis* is distinguished by the shape of its sporophore and capillitium, characterized by the presence of amorphous nodules and deeply reticulated spores. This study expands the knowledge of Neotropical myxomycetes and provides new insights into cultivation methods and ecological interactions.

Introduction

Physarales is a large order of dark-spored myxomycetes, comprising approximately 450 species (Lado 2005-2025), currently divided into two families: Physaraceae and Didymiaceae. The order includes the genera *Didymium* Schrad, the most representative, *Diderma* Persoon, both described at the end of the 18th century (Persoon 1794; Schrad 1797), *Diachea* Fries and *Polyschismium* Corda, formerly *Lepidoderma* de Bary ex Rostaf (García-Martín et al. 2023). The genus *Diderma* currently includes approximately 90 valid species, with *D. globosum* Persoon as the type species (Lado 2005-2025; Novozhilov et al. 2022). It is characterized by a one-, two- or three-layered peridium with granular lime and filamentous capillitia (Persoon 1794; Poulant et al. 2011).

In the past two decades, three species of the genus *Diderma* have been described in Brazil: *D. albo-columella* Bezerra & Cavalcanti (Bezerra et al. 2010), *D. aglomerospora* Barbosa & Cavalcanti (Barborsa et al. 2021) and *D. laiseae* Moreira, Leonardo-Silva & Xavier-Santos (Moreira et al. 2024). In this context, we describe *Diderma brasiliensis*, a new species from Brazil, based on both morphological and phylogenetic evidence. Furthermore, we investigate the species' life cycle and present strategies for cultivating and domesticating phaneroplasmodia – the vegetative phase – which has yielded interesting observations to be presented and discussed, such as the plasmodium's interaction preferences with *Fusarium* cf. *decemcellulare* Brick.

Materials and Methods

Specimens and morphological characterization

Specimens were collected over a six-month period in the Botanical Garden of Anápolis, Goiás, Brazil. The vouchers were deposited in the fungal collection of the fungarium of the Universidade Estadual de Goiás

(HUEG-Fungi) and isotypes sent to the URM herbarium and SP herbarium (Thiers 2025 [updated continuously]).

For macroscopic characterization, sporophores were photographed using a Leica EZ4HD stereoscope, and their size was estimated from the diameter measured at two different points on 50 individuals. The color indication for the characters was based on Kornerup & Wansher (1978) color cards. For the microscopic studies, the sporophore samples were mounted on slides with 4% potassium hydroxide, visualized and photographed using Olympus CX31 and Zeiss Axiolab 5 optical microscope. Spores and capillitium were also observed using a JSM-6610 Scanning Electron Microscope (SEM) (Jeol, Tokyo, Japan) at the High-Resolution Multiuser Microscopy Laboratory (LabMic) at the Universidade Federal de Goiás. Dimensions of were estimated by averaging the measurements from 100 individual structures using Labscope 4.3.2 software (Zeiss).

Cultivation in culture medium and life cycle

For studies on cultivation, domestication, and life cycle of the species, we prepared a spore solution by placing 2 to 3 sporophores into a 2 mL microtube containing 0.7 mL of 0.1% Tween solution. The microtube was shaken manually until the complete disintegration of the sporophores. Spore germination was carried out on 2% water-agar medium in 9 mm Petri dishes, where 30 µL of the spore suspension was inoculated at 4 to 5 equidistant points, avoiding the edges of the plate. The plates were incubated in the dark at 26 ℃ in a BOD chamber. Spore germination was analyzed after 24 h, and myxamoeba were observed using a Zeiss Axiolab 5 optical microscope.

With the plasmodial formation, sub-cultures were performed under two distinct conditions to observe its behavior: (I) on germination paper, kept constantly moist, but without water accumulation at the bottom of the plate; and (II) on 2% water-agar medium. Both cultures were incubated in the dark at 26°C in a BOD chamber. The plasmodium was fed intermittently, according to its apparent activity and movement toward the food source, using oat grains, basidioma of *Favolus* sp. and *Auricularia* sp., and lichens fragments. The mature plasmodia were then sub-cultured in a 2% water-agar medium to keep the plasmodia alive.

Cultures were analyzed every 24 h for up to 15 days, and the behavior of the plasmodium, as well as the development of other life cycle stages, were recorded using a Leica EZ4HD stereomicroscope. During cultivation on water-agar, a species of filamentous fungus emerged and interacted with the plasmodium throughout the observation period. This fungus was isolated on Potato Dextrose Agar (PDA) medium and deposited in the culture collection of the laboratório de Micologia Básica, Aplicada e Divulgação Científica (FungiLab), da Universidade Estadual de Goiás, under the accession number SXS1047.

DNA extraction, PCR amplification and sequencing

Total DNA was extracted according to the CTAB method (Doyle and Doyle 1987; Góes-Neto et al. 2005), with adaptations. For the myxomycete samples, seven whole sporophores were macerated in three

cycles of 90 s each at 3000 rpm using a Micrutube Homogeniser™ (Bead Bug) with three 3 mm glass beads, seven 1 mm silica beads and 600 uL of 2% CTAB buffer. The same process was applied to a fungal sample grown on potato dextrose agar (PDA), with DNA extracted directly from the mycelium. Extraction for both samples followed the standard CTAB protocol. The DNA was eluted in 30 uL of ultrapure H_2O, quantified by fluorometry using the Quantus™ Fluorometer (Promega Corporation, Madison, WI, USA), and subsequently diluted to a final concentration of 20 ng/µL. DNA quality was assessed on a 1% agarose gel, where clear bands were observed for both samples.

Amplification of the first intron-free region of the 18S rRNA and the mitochondrial small subunit (mtSSU) gene in the myxomycete was performed using the primer pairs S2/SU19R (Fiore-Donno et al., 2008; Fiore-Donno et al., 2011) and Kmit_F/Kmit_R (Lado et al, 2022), respectively (Table 1). For the fungal sample, the ITS region was amplified using ITS4/ITS5 primers (White et al. 1990) (Table 1). The thermocycling protocol used for PCR in both organisms followed the parameters listed in Table 1. PCR reactions were carried out in a final volume of 25 µL, containing 12.5 µL of Taq Pol Master Mix Green 2x (Cellco™, Brazil), 0.5 µL of each Primer (10 ng/µL), 1 µL of DNA (diluted to 20 ng/µL), and 10.5 µL of ultra-pure H2O. PCR products were purified and sequenced with the same primers used in the amplification performed in an Applied Biosystems 3730xl DNA Analyzer (MacroGen Ltd., South Korea).

Table 1
Primers and thermocycling protocol utilized in this article.

Region	Primers	F/R	Sequence (5'→3')	Thermocycling protocol
18S rRNA	S2	F	TGGTTGATCCTGCCAGTAGTGT	5 min at 95°C, 36 cycles (30 sec at 95°C, 20 sec at 56°C, 50 sec at 72°C) and 5 min at 72°C
	SU19R	R	GACTTGTCCTCTAATTGTTACTCG	
mtSSU	Kmit_F	F	AGTGTTATTCGTGATGACTGG	5 min at 95°C, 32 cycles (30 sec at 95°C, 1 min at 52°C, 90 sec at 72°C) and 10 min at 72°C
	Kmit_R	R	CGAATTAAACCACATCTCCACC	
ITS fungal	ITS4	F	TCCTCCGCTTATTGATATGC	5 min at 95° C, 25 cycles (45 sec at 95° C, 45 sec at 54° C, 1 min at 72° C) and 10 min at 72° C
	ITS5	R	GGAAGTAAAAGTCGTAACAAGG	

Phylogenetic analyses

Sequence chromatograms were assembled and edited using Staden Package 2.0 (Staden et al. 1998) and compared with the consensus sequences deposited in the GenBank database using BLAST (http://blast.ncbi.nlm.nih.gov/). GenBank sequences with high similarity were extracted and aligned with the present study using the online version of MAFFT (Katoh and Standley 2013); these data were manually inspected using MEGA v.6 (Tamura et al. 2013). The genus *Lamproderma* Rostaf was used as an outgroup in phylogenetic analyses (García-Martín et al. 2023). The sequences generated in this study have been deposited in GenBank and are available in (Table 2) along with the other sequences used in the analyses.

Phylogenetic analyses were inferred with Maximum Likelihood (ML) and Bayesian Inference (BI) performed in W-IQ-TREE (Kalayaanamoorthy et al. 2017) and MrBayes v. 3.2 (Ronquist and Huelsenbeck 2003), respectively, under the substitution model SYM + I + G for the 18S rRNA region and GTR + G for the mtSSU region estimated based on the Akaike Information Criterion (AIC). ML was determined with branch support (BS) inferred by 1000 bootstrap replications and Ultrafast bootstrap (UB). BI was performed with 6 million generations, with convergence verified in TRACER v. 1.7.1 (Rambaut et al. 2018), and the first 25% of the resulting trees were discarded as burn-in; Bayesian posterior probabilities (PP) were calculated from the remaining sampled trees. Significant support was assumed for nodes with BS and UB ≥ 70% and PP ≥ 0.95.

The fungal sequences were compared with those available in the GenBank database using the BLAST search tool (http://blast.ncbi.nlm.nih.gov/) to identify the isolate, based on similarity percentage. Values above 94% were considered to belong to the same genus, and above 97% to the same species (Li et al. 2016).

Table 2
Specimens along with GenBank accession numbers used in the phylogenetic analysis. The sequences obtained in this study are marked in **bold**.

Species	Locality	Voucher	GenBank accesscode	
			18S rRNA	mtSSU
Diderma cor-rubrum	Russia	LE302473	OP621216	OR769428
Diderma cor-rubrum	Russia	MYX11340	OP621217.1	OR769459.1
Diderma aurantiacum	Russia	LE302633	OQ312104.1	OQ316576.1
Diderma aurantiacum	Russia	LE286478	OQ312103.1	OQ316575.1
Diderma tigrinum	USA	SLS17578	OP621309.1	OP616644.1
Diderma tigrinum	Russia	MYX17121	-	OR769436.1
Diderma globosum	Russia	LE325799	MZ604992.1	OR769432.1
Diderma globosum	Russia	LE325793	MZ604991.1	OP616550.1
Diderma globosum	Russia	LE325132	MZ604989.1	OR769430.1
Diderma crustaceum	China	HMJAU M20008-2	PP165432.1	-
Diderma crustaceum	China	HMJAU M20009-2	PP165434.1	-
Diderma niveum	Argentina	MA-Fungi 78780	MW240313.1	MW240172.1
Diderma niveum	Argentina	MA-Fungi 78779	MW240312.1	MW240171.1
Diderma ochraceum	Germany	sc24091	MZ604997.1	OR769434.1
Diderma ochraceum	Czech Republic	sc24049	MZ604996.1	OR769433.1
Diderma savannica	Brazil	HUEG20149		
Diderma effusum	China	HMJAU60270	OQ822775.1	-
Diderma deplanatum	China	HMJAU60234	OQ822781.1	-
Diderma deplanatum	Russia	LE317502a	PP099460.1	PP097332.1
Diderma saundersii	China	HMJAU60249	OQ822785.1	-
Diderma saundersii	China	HMJAUM20027-1	PP165461.1	-
Polyschismium chailletii	Germany	sc31567	PP383399.1	-
Polyschismium chailletii	Germany	sc34152	PP383739.1	-
Diachea subsessilis	Russia	MYX14316	MZ005925.2	OR769427.1

Species	Locality	Voucher	GenBank accesscode	
Diachea subsessilis	China	HMJAUM10075	PP795191.1	PP833138.1
Diachea subsessilis	Russia	LE325164	MZ005926.2	OR769426.1
Diachea leucopodia	China	HMJAUM10005	PP795183.1	PP833130.1
Diachea leucopodia	Peru	MA-Fungi 90990	MG963646.1	MG963551.1
Diachea bulbillosa	Russia	LE297619	OP621206.1	OR769456.1
Diachea bulbillosa	Russia	MYX11336	OP621207.1	PP501432.1
Diachea bulbillosa	China	HMJAUM10037	PP795178.1	PP833125.1
Diachea muscorum	Russia	MYX12433	OR769402.1	OR769421.1
Diachea muscorum	France	MM28650	OP650744.1	OP646254.1
Didymium melanospermum	Spain	MA-Fungi 91238	MG963668.1	MG963577.1
Didymium melanospermum	Spain	MA-Fungi 62790	MG963667.1	MG963577.1
Didymium operculatum	Chile	MA-Fungi 80820	MG963670.1	-
Didymium operculatum	Chile	MA-Fungi 74050	MG963669.1	MG963578.1
Lamproderma spinulosporum	-	MM32506	JQ031996.1	-
Lamproderma ovoideum	Russia	LE285863	JQ812669.1	-

Results

Phylogenetic analyses

BLASTn analysis of the 18S rRNA region revealed 92.6% similarity with *D. crustaceum* Peck, while the mtSSU region showed 90.68% similarity with *D. cor-rubum* Macbr. The sequences obtained were compared with those of other species within the family Didymiaceae, resulting in a final matrix consisting of four genera, 39 species, and two outgroup sequences (Table 2). The final alignment consisted of 585 characters for the 18S rRNA region and 468 for the mtSSU region, including gaps. BI analysis resulted in an average standard deviation of split frequencies of 0.007501. The ML and BI analyses returned visually congruent tree topologies. Therefore, only the ML tree is shown (Fig. 4). Based on the phylogenetic analysis, *D. brasiliensis* formed a strongly supported clade (BS = 100, UB = 100, PP = 1) with *D. crustaceum* and *D. cor-rubrum.*

Taxonomy

Diderma brasiliensis Toschi, Leonardo-Silva & Xavier-Santos, sp. nov. (Fig. 2–4)

MycoBank: MB858520

GenBank

18S rRNA = PV389897; mtSSU = PV 611069.

Etymology

From the Latin *brasiliensis*, meaning “from Brazil” or “Brazilian”, the epithet refers to the species' country of origin.

Typification: BRAZIL. GOIÁS: Anápolis, Botanical Garden 16°20'22‘S 48°56'25’W, on rotting wood waste, 08 Nov 2024, Toschi LA 118 (holotype HUEG20152/SP 529304/URM 95913).

Material examined: BRAZIL. GOIÁS: Anápolis, Botanical Garden 16°20'21‘S 48°56'26’W, on rotting wood waste, 6 Apr 2024, Toschi LA 108 (HUEG20149); BRAZIL. GOIÁS: Anápolis, Botanical Garden 16°20'21‘S 48°56'26’W, on *Epipremnum aureum* leaf and undetermined plant residues, 4May 2024, Toschi LA 115 (HUEG20150).

Description

Phaneroplasmodium white (1A1) (Fig. 5E–G); When fruiting begins, the immature sporophores are dull lilac (16C3) (Fig. 2A), becoming white (1A1) to greyish brown (1B1) when mature with 0.4–0.8 mm in diameter. Peridium double composed of a thin, hyaline outer layer and a white inner layer (1A1) formed by calcareous granules (Fig. 4D–F). Hypothallus white, dense and membranous (1A1). Columella white (1A1), 0.1–0.3 mm, composed of calcareous granules of 0.03–1.7 µm. Spores globose or subglobose, dark brown (7F4), (8.2) 10.3–11.5 (13.04) × (8.7) 9.5–10.0 (14.5) µm in diameter (including the reticulum), with reticula (0.5) 1.9–2.5 (3.1) µm thick (Fig. 3A, B; 4 A, B). Capillitium brown and tortuous, (1.2)1.5–3.4(5.1) µm, with nodular insets (Fig. 3C-G; Fig. 4C, E) of variable size and arrangement, measuring approximately (1.4) 1.6–3.5 (8.4) µm, anastomosed near the end (Fig. 3C, E, G). The capillitium is attached perpendicularly between the columella and the peridium, becoming more hyaline when close to close to its attachment points (Fig. 2G).

Substrate and habitat

Diderma brasiliensis was found abundantly on the trunks of dead trees that had fallen to the ground and were already in an advanced state of decomposition, on leaf litter and on the living stems and leaves of climbing plant *Epipremnum aureum* (Linden & André) G.S.Bunting.

Cultivation and life cycle

Spore germination began within 10 h of inoculation. Myxamoeba (Fig. 5A) were observed to be active within the first 20 h, preying on bacilliform organisms (Fig. 6C). The first zygote (Fig. 5C) was observed within two days, and the young plasmodium (Fig. 5D-F) became visible under the stereoscope within

eight days. The plasmodium was white, compact, and with advancing edges, where protoplasmic streaming was observed under an optical microscope. As soon as the first zygotes appeared, some were observed engulfing myxamoeba, which enables the phagocytosis of smaller cells. Additionally, young plasmodia were observed to ingest entire ungerminated spores (Supplementary Vid. 1), presumably using them as a nutrient source.

At this point, the plasmodium was fed small fragments of autoclaved oat grains. After further growth, it was transferred to a humid chamber and fed with whole oat flakes. To induce fruiting, the plate was exposed to natural ambient light, and two to three small fragments of autoclaved wood were placed in the plate, which the plasmodium climbed and where it eventually fruited (Fig. 5H).

The species has aggregated fruiting; however, in some cases, fruiting was observed in the moist chamber with isolated formation of sporophores. In these cases, the peridium and columella were found to be poorly developed or absent, resulting in a spore mass with intertwined capillitia that did not follow the typical orientation of the columella and peridium. We believe that this condition is due to chemical stress or microbial activity that compromises the plasmodium development. Another possible factor is nutritional deficiency, caused by a limited quantity and diversity of available food. To address this, we provided the plasmodium with food sources more representative of its natural environment, including small fragments of lichens, and dehydrated basidiomata of the fungi *Favolus* sp. and *Auricularia* sp., all previously autoclaved. Under this varied diet, the plasmodium exhibited improved development.

The water-agar cultures were constantly contaminated by *Fusarium* cf. *decemcellulare* (Fig. 7A), which was partially identified with a corresponding sequence using the BLASTn tool, showing 99.64% similarity with the ITS region. We believe that the sporophores of *D. brasiliensis* were contaminated in the field by conidia of this fungus, as cultures of other myxomycete species maintained under the same laboratory conditions did not show its presence. Contamination was noticeable to the naked eye since the first days of cultivation, initially appearing as small magenta spots at the inoculation site and expanding radially over the surface of the culture medium. In the presence of the fungus, the plasmodium changed its color from the characteristic white to a gradually purplish tone, eventually becoming orange when mature (Fig. 7C). This color change may be due to the incorporation of fungal metabolites or even to the phagocytosis of the fungus by the plasmodium. A certain degree of attraction between the plasmodium and the fungus was also observed, reinforcing the possibility of a predatory relationship.

In cultures without fungal contamination, the plasmodium showed normal development and maintained its typical color, just as when the plasmodium with the alteration was transferred to another plate with new culture medium (Fig. 7D and E), its color gradually returned to the conventional white (Fig. 7E). Although fungal contamination can hinder myxomycete growth—particularly during the myxamoeba stage, this effect was not evident in the present study. Due to the low nutrient content of the water-agar medium, the growth of *F.* cf. *decemcellulare* was initially limited; however, over time, its colonization became more extensive.

Discussion

Diderma brasiliensis was recorded at different sites in the Anápolis Botanical Garden. This urban green space covers an area of around 25,000 m² and is crossed by the Ipiranga stream, whose bed is dammed within the park. The vegetation of the park includes native species from the Cerrado and Atlantic Forest, including large trees. These features give rise to a mosaic of microhabitats characterized by shading, high moisture and abundant organic matter, like as dense litter, ideal conditions for the development of the myxomycetes (Stephenson & Rojas 2017). The species described here is morphologically distinguished by its globose to subglobose sporophores, nodular capillitium and deeply reticulate spores. These characteristics set it apart from closely related species such as D. *cor-rubrum* T. Macbr. and *D. crustaceum* Peck, which form a clade with *D. brasiliensis* in our phylogenetic analysis but differ in spore ornamentation and capillitial architecture.

D. brasiliensis also shares traits with *D. subdictyospermum* Rostaf, particularly the conspicuous spore spore reticula and robust, anastomosing capillitia (vide Liy and Chen 1999; Sánchez et al. 2002; Li et al. 2024; Yamamoto et al. 2006). However, *D. brasiliensis* can be easily differentiated by its more tortuous capillitia, a higher frequency of amorphous nodules, and slightly smaller spores that lack subreticula.

Phylogenetic inference based on 18S rRNA and mtSSU sequences confirmed the distinct position of *D. brasiliensis* from known taxa, reinforcing the importance of integrating morphological and molecular data in species delimitation (Fiore-Donno et al., 2008; García-Martín et al., 2023). However, the latter lacks molecular data in public repositories, precluding its inclusion in the phylogenetic tree and reinforcing the novelty of Notably, *D. subdictyospermum* lacks molecular data in public repositories, which precluded its inclusion in our phylogenetic tree and underscores the novelty of our findings.

Importantly, our study goes beyond taxonomic delineation by documenting the complete life cycle of *D. brasiliensis* under controlled conditions, a rare approach in the literature, despite its importance for understanding species biology (Borg Dahl et al. 2019; Poulain et al. 2011). Observations of phagocytosis of myxamoebae by early formed zygotes, and of ungerminated spores by juvenile plasmodia, highlight trophic plasticity and suggest adaptive mechanisms such as predation and autophagy. These behaviors may confer ecological advantages under resource-limited or competitive environments (Bloomfield 2018. Fiore-Donno et al. 2011) and raise new questions about the survival strategies of myxomycetes.

We also observed the assimilation by the plasmodium of pigment from *Fusarium* cf. *decemcellulare*. The plasmodium appeared attracted to fungal hyphae and underwent visible color changes, indicating a possible predatory interaction. This observation opens promising avenues for biotechnological research, particularly concerning the potential of myxomycetes in fungal control, a field still underexplored within protistology. This is especially relevant considering that the genus *Fusarium* includes species with high phytopathogenic potential (Geiser et al., 2013). Although scarcely documented in the literature, myxomycete–fungus interactions such as those observed here may represent a novel and valuable line of investigation for the development of biocontrol strategies.

Finally, the ability to cultivate the species, maintain it in culture, and induce sporulation under laboratory conditions represents a methodological advance that facilitates experimental designs, genomic analysis and studies on physiological and behavioral myxomycete research. This is particularly relevant given the underrepresentation of Neotropical taxa in molecular databases such as GenBank and MycoBank (Fiore-Donno et al., 2008; García-Martín et al., 2023). By including DNA sequences from *D. brasiliensis*, this study contributes to expanding the known myxodiversity and mitigating gaps in phylogenetic and biogeographic studies.

Conclusion

This study describes *Diderma brasiliensis* as a new species of myxomycete, supported by both morphological distinctiveness and robust phylogenetic evidence. Beyond contributing to the taxonomy of the genus *Diderma*, the research offers original insights into its life cycle, trophic behavior, and ecological interactions, including signs of autophagy and a possible predatory relationship with a fungus.

The successful cultivation and induction of sporulation under controlled laboratory conditions represent a methodological advancement, paving the way for future studies on the physiology, genomics, and experimental ecology of this species. Moreover, the deposition of DNA sequences in public databases helps address the underrepresentation of tropical taxa in molecular repositories, thereby strengthening phylogenetic and biogeographic analyses of myxomycetes and contributing to global efforts to map this biodiversity.

Altogether, this work highlights the ecological and scientific relevance of *D. brasiliensis* and reinforces the importance of continuing to explore the rich, yet still poorly documented, myxomycete diversity of the Neotropics.

Declarations

Acknowlegments

We are grateful to the Coordenação de Aperfeiçoamento de Pessoal de Ensino Superior (CAPES), for the funding (Convênio n° 21-2022) and for Master's scholarship provided to LAT; to the Conselho Nacional de Desenvolvimento Científico e Tecnológico (CNPq) and to Fundação de Amparo à Pesquisa do Estado de Goiás (FAPEG) for providing the PDJ scholarship to LL-S, and to CNPq for the productivity grants to SX-S.

Ethical approval:

Not applicable

Consent to participate:

Not applicable

Consent to publish:

All authors authorise publication

Competing interests:

The authors declare no competing interests.

Funding:

Not applicable

Author contributions:

LAT: specimen collection, morphological description, molecular biology and phylogeny, writing; LLS: writing, molecular biology and phylogeny; SXS: writing, morphological description.

Data availability statement:

Voucher is deposited in Fungarium HUEG. The sequences generated in this study are deposited in NCBI GenBank (https://www.ncbi.nlm.nih.gov/genbank/).

References

1. Alfaro ME, Zoller S, Lutzoni F (2003) Bayes or bootstrap? A simulation study comparing the performance of Bayesian Markov chain Monte Carlo sampling and bootstrapping in assessing phylogenetic confidence. Mol Biol Evol. 20(2):255–266. https://doi.org/10.1093/molbev/msg028
2. Barbosa DÍ, Melo TEO, Brayner FA, Cavalcanti LH (2021) *Diderma aglomerospora* (Didymiaceae, Physarales, Myxomycetes), a new species from Brazil. Phytotaxa. 494(2):231–236. https://doi.org/10.11646/phytotaxa.494.2.6
3. Bezerra ACC, Cavalcanti LH (2010) *Diderma albo-columella* (Myxomycetes), a new species in the Brazilian Atlantic Forest. Rodriguésia. 61(1):105–108. https://doi.org/10.1590/2175-7860201061111
4. Bloomfield G (2018) The evolution of ogres: cannibalistic growth in giant phagotrophs. bioRxiv. 262378. https://doi.org/10.1101/262378

5. Borg Dahl M, Brejnrod AD, Russel J, Sørensen SJ, Schnittler M (2019) Different degrees of niche differentiation for bacteria, fungi, and myxomycetes within an elevational transect in the German Alps. Microb Ecol. 78(3):764–780. https://doi.org/10.1007/s00248-019-01347-1
6. Fiore-Donno AM, Meyer M, Baldauf SL, Pawlowski J (2008) Evolution of dark-spored Myxomycetes (slime-molds): molecules versus morphology. Mol Phylogenet Evol. 46:878–889. https://doi.org/10.1111/j.1550-7408.2005.00032.x
7. Fiore-Donno AM, Novozhilov YK, Meyer M, Schnittler M (2011) Genetic structure of two protist species (Myxogastria, Amoebozoa) suggests asexual reproduction in sexual amoebae. PLoS ONE. 6(8):e22872. https://doi.org/10.1371/journal.pone.0022872
8. García-Martin JM, Zamora JC, Lado C (2023) Multigene phylogeny of the order Physarales (Myxomycetes, Amoebozoa): Shedding light on the dark-spored clade. Persoonia. 51:89–124. https://doi.org/10.3767/persoonia.2023.51.02
9. Geiser DM, Aoki T, Bacon CW, Baker SE, Bhattacharyya MK, Brandt ME, Zhang N (2013) One fungus, one name: defining the genus Fusarium in a scientifically robust way that preserves longstanding use. Phytopathology. 103(5):400–408. https://doi.org/10.1094/PHYTO-07-12-0150-LE
10. Kalayaanamoorthy S, Minh BQ, Wong TKF, Von Haeseler A, Jermiin LS (2017) ModelFinder: fast model selection for accurate phylogenetic estimates. Nat Methods. 14(6):587–589. https://doi.org/10.1038/nmeth.4285
11. Katoh K, Standley DM (2013) MAFFT Multiple Sequence Alignment Software Version 7: Improvements in Performance and Usability. Mol Biol Evol. 30(4):772–780. https://doi.org/10.1093/molbev/mst010
12. Kornerup A, Wanscher JH (1978) Methuen Handbook of Colour. 3ª ed. Methuen, Londres
13. Lado C, Treviño-Zevallos I, García-Martín JM, Wrigley de Basanta D (2022) *Diachea mitchellii*: a new myxomycete species from high elevation forests in the tropical Andes of Peru. Mycologia. 114(4):798–811
14. Li P, Wu Z, Liu T, Wang Y (2016) Biodiversity, phylogeny, and antifungal functions of Endophytic Fungi associated with *Zanthoxylum bungeanum*. Int J Mol Sci. 17:1541. https://doi.org/10.3390/ijms17091541
15. Li X, Tuo Y, Hu J, Li Y, Dai D, Sossah FL, Wang J, Guo Y, Liu S, Ma H, Zhang B, Li X, Li Y (2024) New species, new records, and common species of *Diderma* (Physarales, Didymiaceae) from China. Microbiol Spectr. 0:e01265-24. https://doi.org/10.1128/spectrum.01265-24
16. Liu CH, Chen YF (1999) Myxomycetes of Taiwan—XII. New records and newly rediscovered species. Taiwania. 44(3):368–375. https://doi.org/10.6165/tai.1999.44(3).368
17. Moreira IC, Leonardo-Silva L, Xavier Santos S (2025) *Diderma laiseae* (Didymiaceae, Physarales), a new species of Myxomycetes from Brazil. Phytotaxa. 682(2). https://doi.org/10.11646/phytotaxa.682.2.8
18. Novozhilov YK, Rollins AW, Shchepin ON, Schnittler M (2022) Ecology and distribution of Myxomycetes. Em: Rojas C, Stephenson SL (orgs.) Myxomycetes: Biology, Systematics,

Biogeography, and Ecology. 2ª ed. Academic Press, pp. 325–376. https://doi.org/10.1016/B978-0-12-824281-0.00010-5

19. Persoon CH (1794) Neues Magazin für die Botanik in ihrem ganzen Umfange - *Diderma*. 1:89. p. 336
20. Poulain M, Meyer M, Bozonnet J (2011) Les Myxomycetes. Fédération mycologique et botanique Dauphiné-Savoie, Sévrier
21. Prikhodko IS, Shchepin ON, Bortnikova NA, Novozhilov YK, Gmoshinskiy VI, Moreno G, Lopez-Villalba A, Stephenson SL, Schnittler M (2023) A three-gene phylogeny supports taxonomic rearrangements in the family Didymiaceae (Myxomycetes). Mycol Prog. 22:11. https://doi.org/10.1007/s11557-022-01858-1
22. Sánchez A, Moreno G, Illana C (2002) *Diderma cristatosporum*, a nivicolous Myxomycete from Spain. Persoonia. 17(4):643–647
23. Schrader HA (1797) Nova Genera Plantarum - *Didymium*. p. 1–32. Disponível em: https://www.biodiversitylibrary.org/page/12930554
24. Staden R, Beal KF, Bonfield JK (1998) The Staden package. Em: Misener S, Krawetz SA (orgs.) Bioinformatics Methods and Protocols. The Humana Press, pp. 115–130
25. Stephenson SL, Rojas C (2017) Myxomycetes: Biology, Systematics, Biogeography and Ecology. Academic Press
26. Tamura K, Stecher G, Peterson D, Filipski A, Kumar S (2013) MEGA6: Molecular evolutionary genetics analysis version *6.0*. Mol Biol Evol. 30(12):2725–2729. https://doi.org/10.1093/molbev/mst197
27. Yamamoto Y, Kimura T, Degawa Y (2006) A tropical slime mold, *Diderma subdictyospermum,* new to Japan. Bull Kanagawa Prefect Mus Nat Sci. (35):33–34

Figures

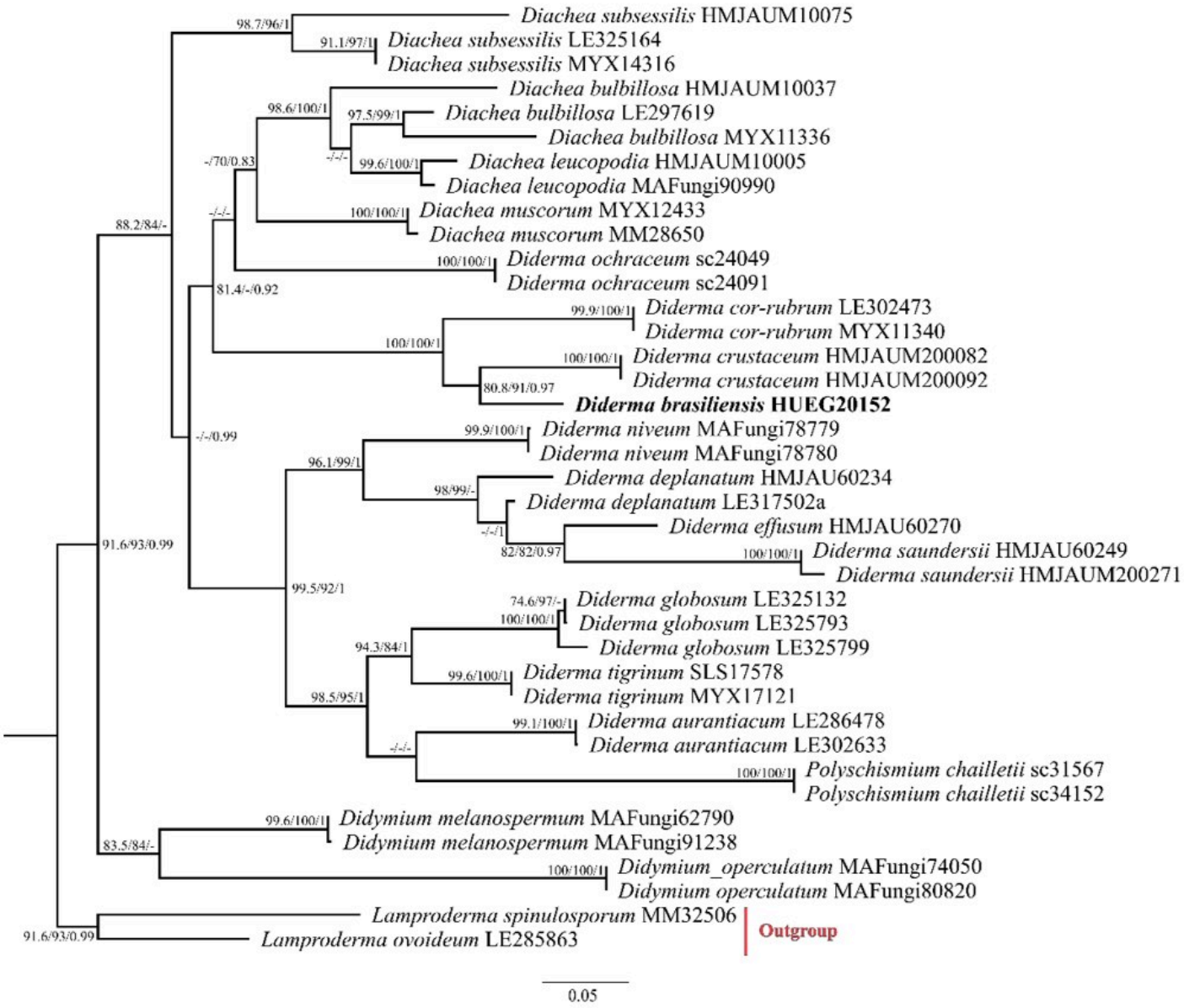

Figure 1

Maximum likelihood tree inferred from concatenated 18S rRNA and mtSSU sequences for the phylogenetic relationship of the Didymiaceae family, with members of the *Lamproderma* genus as an outgroup. Supports are shown for maximum likelihood ultrafast bootstrap replicates (UB)/branch support (BS)/Bayesian Posterior probabilities (PP), respectively. Sequence of *Diderma brasiliensis* is in **bold**

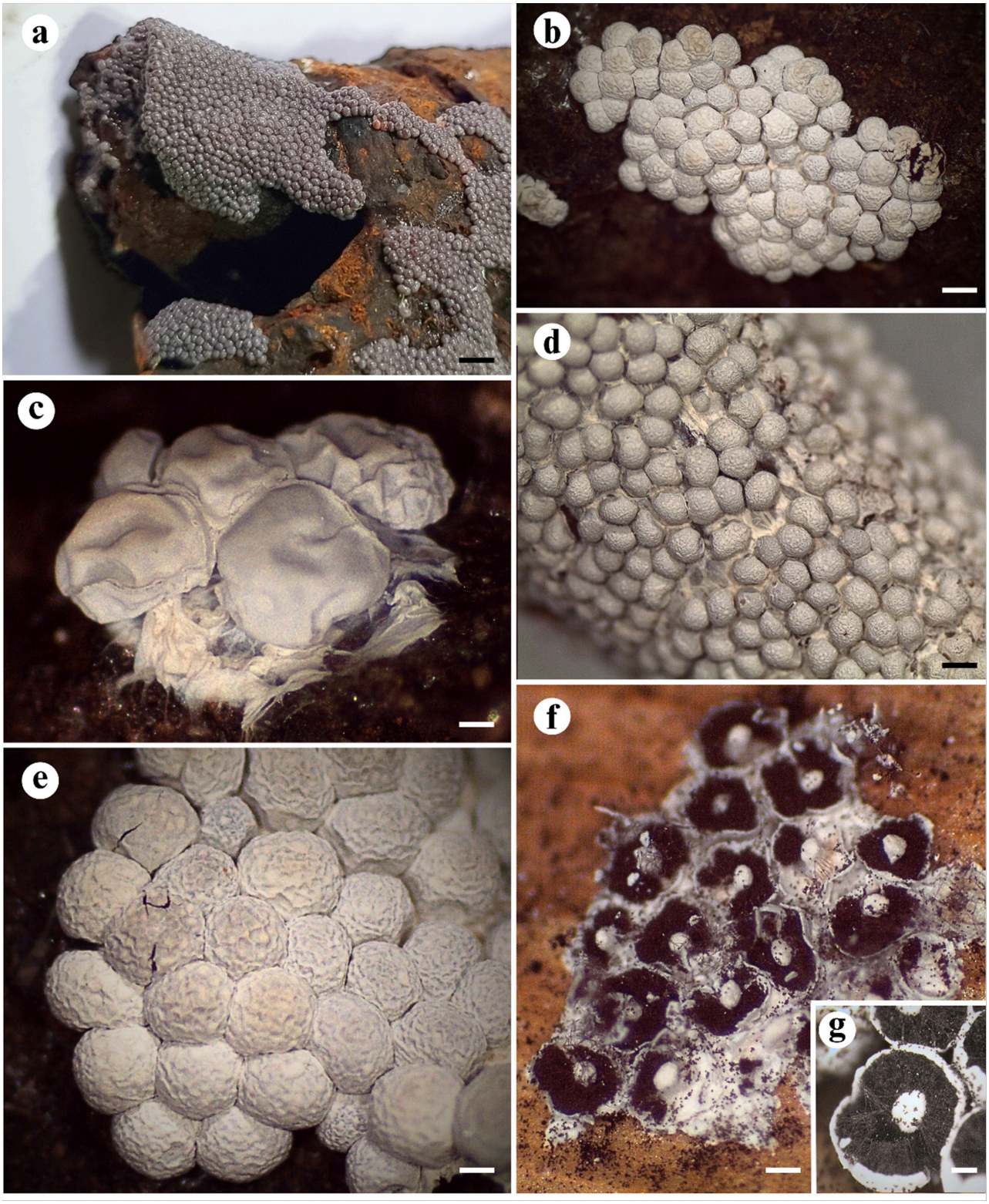

Figure 2

Diderma brasiliensis sporophores (Toschi LA 118, HUEG2052). (A–E) Intact sporophores. (F, G) Sporophores with apical dehiscence, exposing the columella, spore mass, and capillitium network (Toschi LA 117, HUEG 20151). Bars: A = 3 mm; B, D = 0.5 mm; C = 0.25 mm; E = 0.3 mm; F = 0.2 mm; G = 0.05 mm

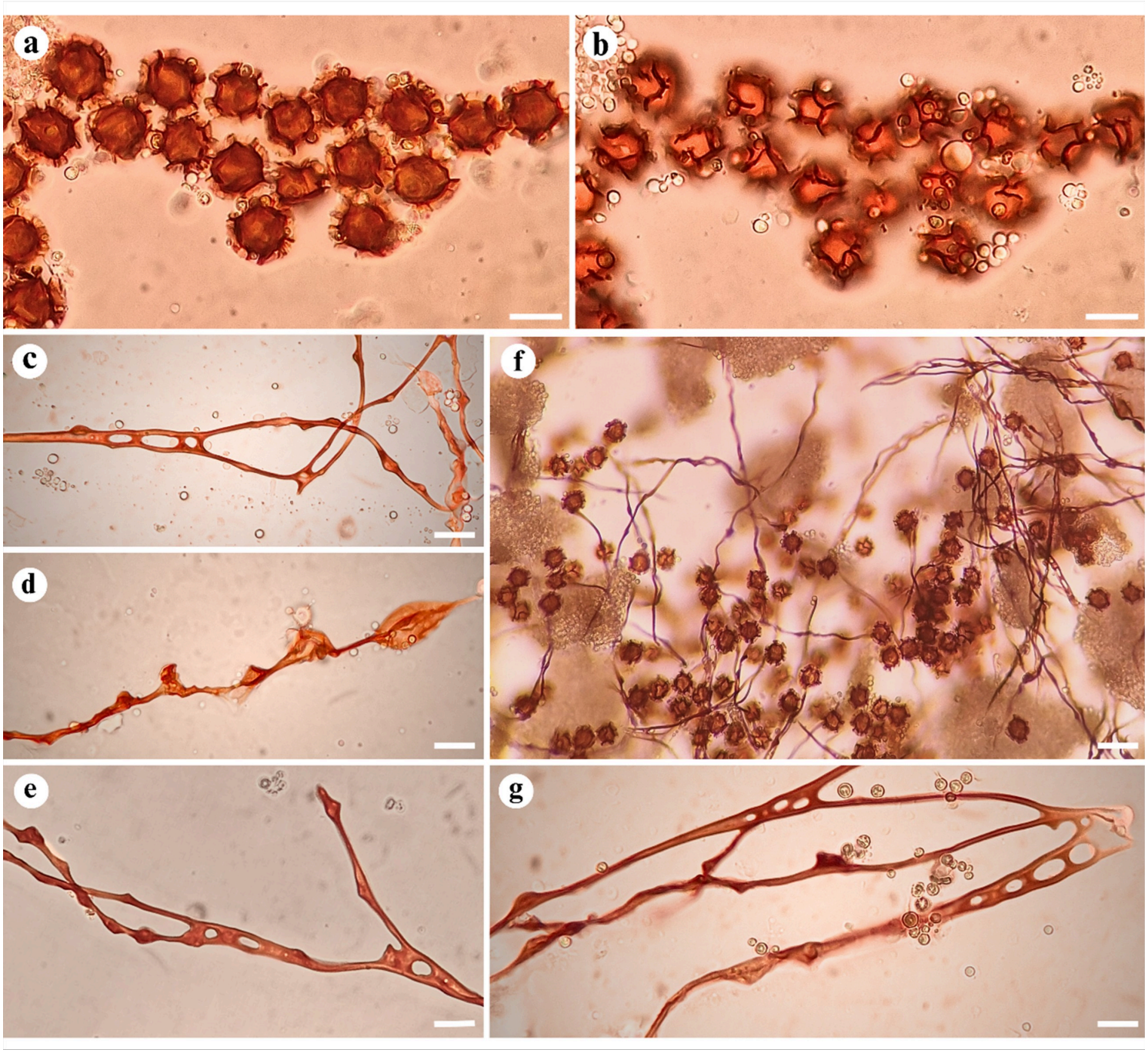

Figure 3

Microstructures of *Diderma brasiliensis* (Toschi LA 118, HUEG20152). (A, B) Spores and calcareous granules in different foci. (C–E, G) Capillitium. (F) General view of the spores and capillitium. Bars: A, B = 10 μm; C, D, E, G = 4.5 μm; F = 15 μm

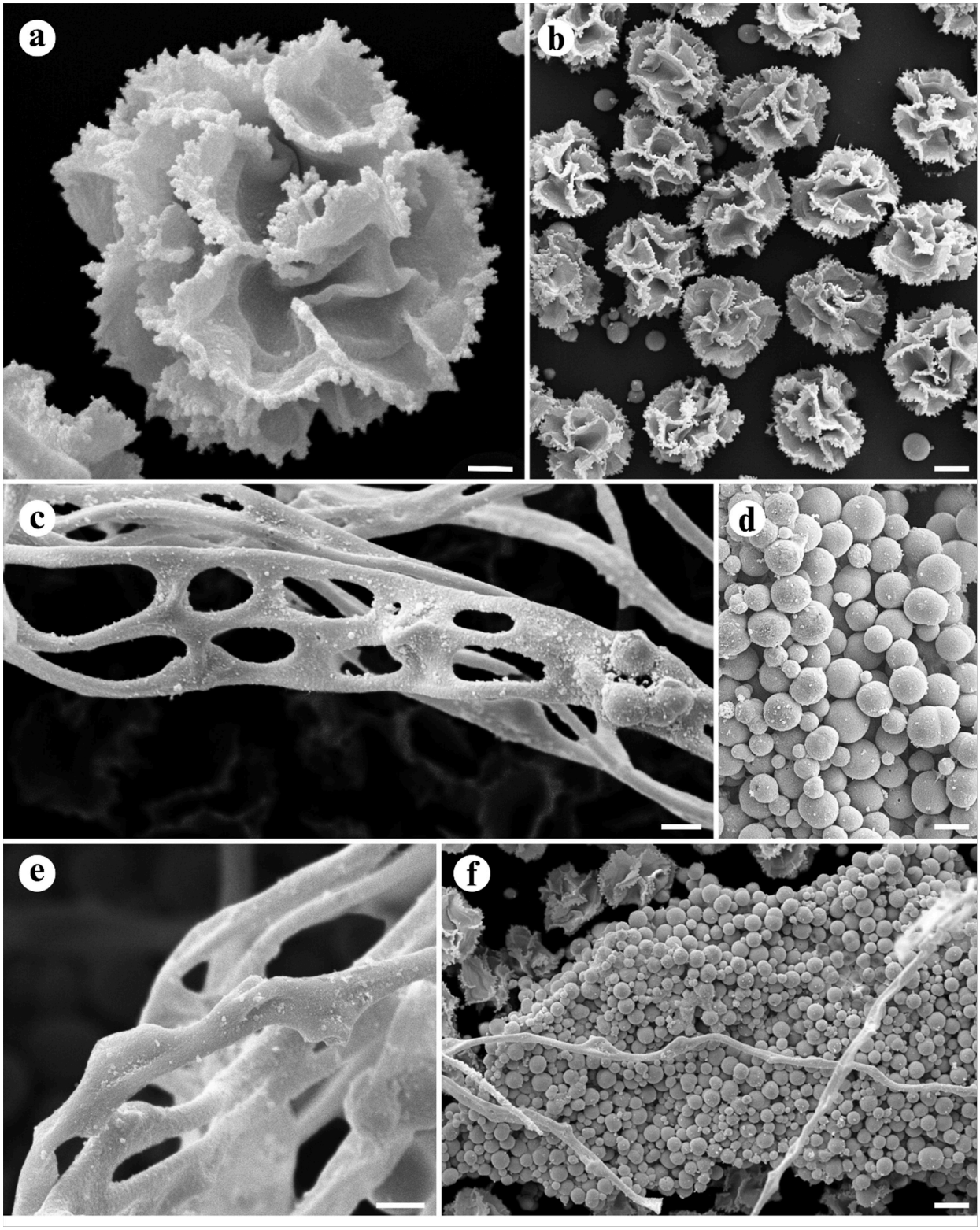

Figure 4

Scanning electron micrographs of *Diderma brasiliensis* (Toschi LA 118, HUEG 20152). (A) Spore. (B) Spores in aggregation. (C) Capillitium. (D) Calcareous granules. (E) Capillitium. (F) Fragment of the peridium showing its layer of calcareous granules. Bars: A = 1 µm; B = 4 µm; C = 2 µm; D = 1 µm; E = 1.5 µm; F = 3 µm

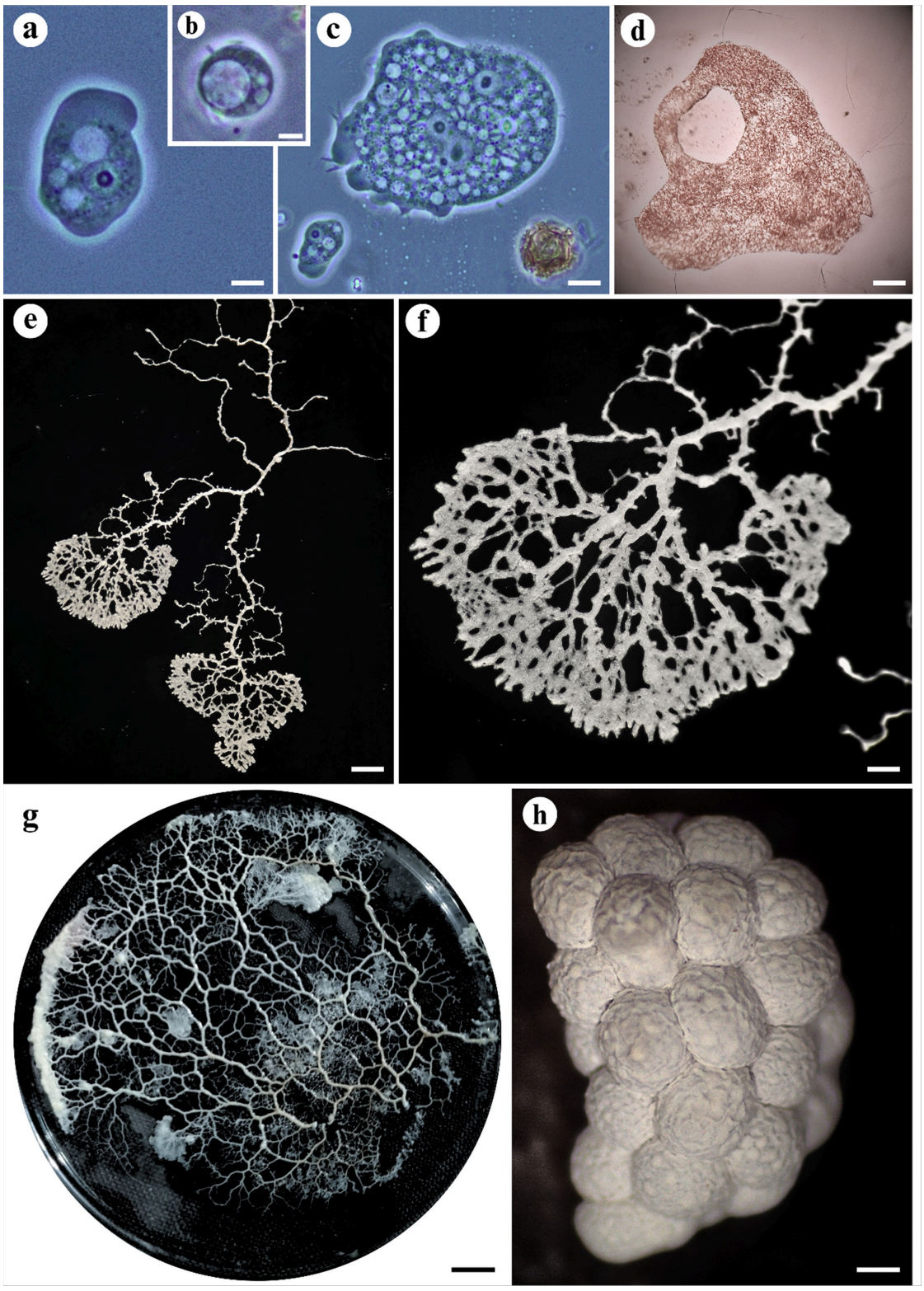

Figure 5

Life cycle of *Diderma brasiliensis*. (A) Myxamoeba of 20 h in intense activity. (B) Unicellular cyst. (C) Zygote of 2 d in intense activity (time-lapse video accelerated 15 times available in Supplementary Vid. 2). (D) Young plasmodium. (E–G). Plasmodium already developed. (H) Sporophores obtained in moist chamber. Bars: A, B = 5 µm; C = 10 µm; D = 0.2 mm; E = 0.5 mm; F = 0.05 mm; G = 1 cm; H = 0.2 mm

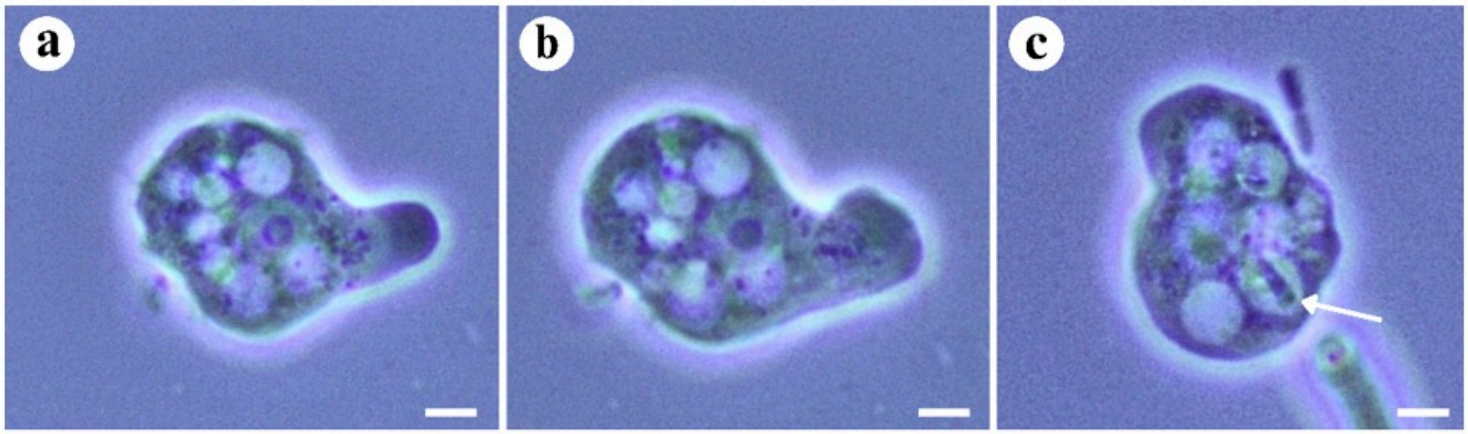

Figure 6

Myxamoeba of approximately 24 h at different times. (A, B) showing emission of pseudopod, with 5 seconds apart between the photos; (C) with bacilliform organisms in digestive vesicle (arrow). Bars: A–C = 1.5 µm

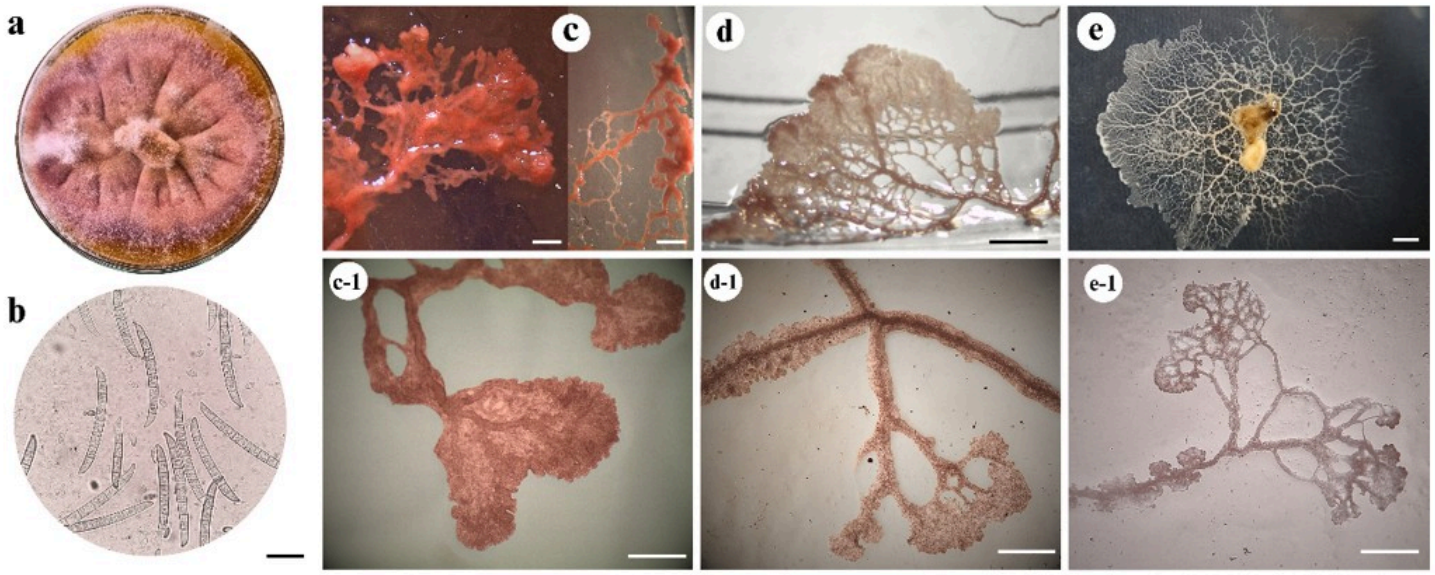

Figure 7

Cultures in the presence of the fungus *Fusarium* cf. *decemcellulare*. (A) Colony of *F. decemcellulare*in PDA medium; (B) Conidia of *F. decemcellulare*; (C) Plasmodium in contaminated with the fungus water agar culture; (D) Plasmodium transferred to new water agar culture medium after ca. 48 h; (E) The same plasmodium after 7 days. B= 15 µm; C, D= 1 mm; E= 0.5 cm; C-1=0.5 mm; D-1, E-1= 1 mm

Supplementary Files

This is a list of supplementary files associated with this preprint. Click to download.

- VIDEO1MACRO.mp4
- VIDEO2MICRO.mp4